MMHT updates, LHC data and QED PDFs

Robert Thorne

September 6th, 2017

University College London

With contributions from Lucian Harland-Lang, Alan Martin and Ricky Nathvani

I will briefly recall recent fits and PDFs to new collider data (nearly all LHC).

Also introduce first results on PDFs with QED corrections, with input photon based on the LUXqed photon. (Manohar *et. al PRL 117, 242002 (2016),* arXiv:1708.01256.)

Other ongoing developments on code restructure, LHC jets, extended parameterisation *etc.* not reported here.

MMHT preliminary set - fit to new hadron collider (mainly LHC) data

We now also fit to high rapidity W, Z data from LHCb at 7 and 8 TeV, $W + c$ jets from CMS, which constrains strange quarks, high precision CMS data on $W^{+,-}$ rapidity distributions, and also the final e asymmetry data from D0..

	no. points	NLO χ^2_{pred}	NLO χ^2_{new}	NNLO χ^2_{pred}	NNLO χ^2_{new}
$\sigma_{t\bar{t}}$ Tevatron +CMS+ATLAS	18	19.6	20.5	14.7	15.5
LHCb 7 TeV $W + Z$	33	50.1	45.4	46.5	42.9
LHCb 8 TeV $W + Z$	34	77.0	58.9	62.6	59.0
LHCb 8TeV e	17	37.4	33.4	30.3	28.9
CMS 8 TeV W	22	32.6	18.6	34.9	20.5
CMS 7 TeV $W + c$	10	8.5	10.0	8.7	8.0
D0 e asymmetry	13	22.2	21.5	27.3	25.8
total	3738/3405	4375.9	4336.1	3741.5	3723.7

Predictions good, and no real tension with other data when refitting, i.e. changes in PDFs relatively small.

At NLO $\Delta\chi^2 = 9$ for the remainder of the data and at NNLO $\Delta\chi^2 = 8$.

When couplings left free at NLO $\alpha_S(M_Z^2)$ stays very close to 0.120 but at NNLO $\alpha_S(M_Z^2)$ marginally above 0.118, higher than MMHT2014.

New data sets for fit – $W + c$ differential distributions.

Direct constraint on strange quark - $s + g \to W + c$.

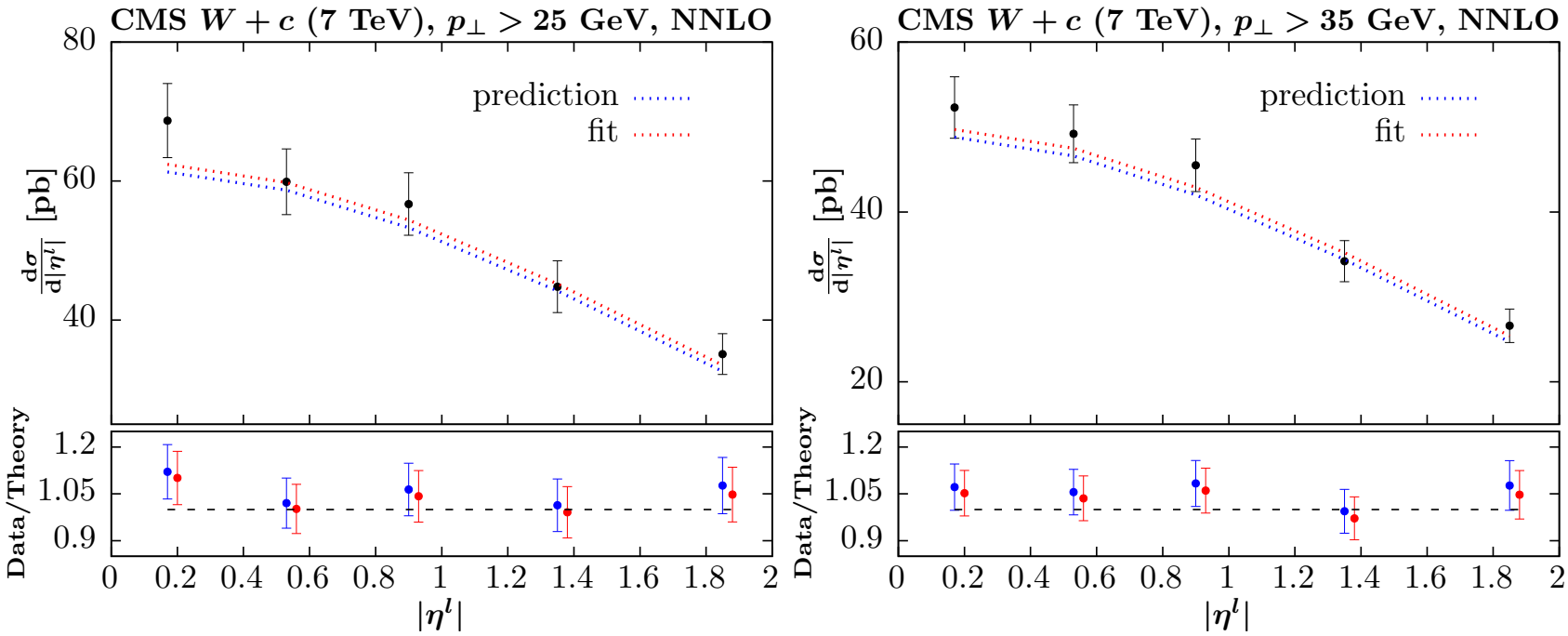

Data on plot use uncertainties added in quadrature.

Very little change after fit. By eye comparison looks worse, but slightly better when covariance matrix used (as in fit).

Included some more up-to-date results on $\sigma_{\bar{t}t}$.

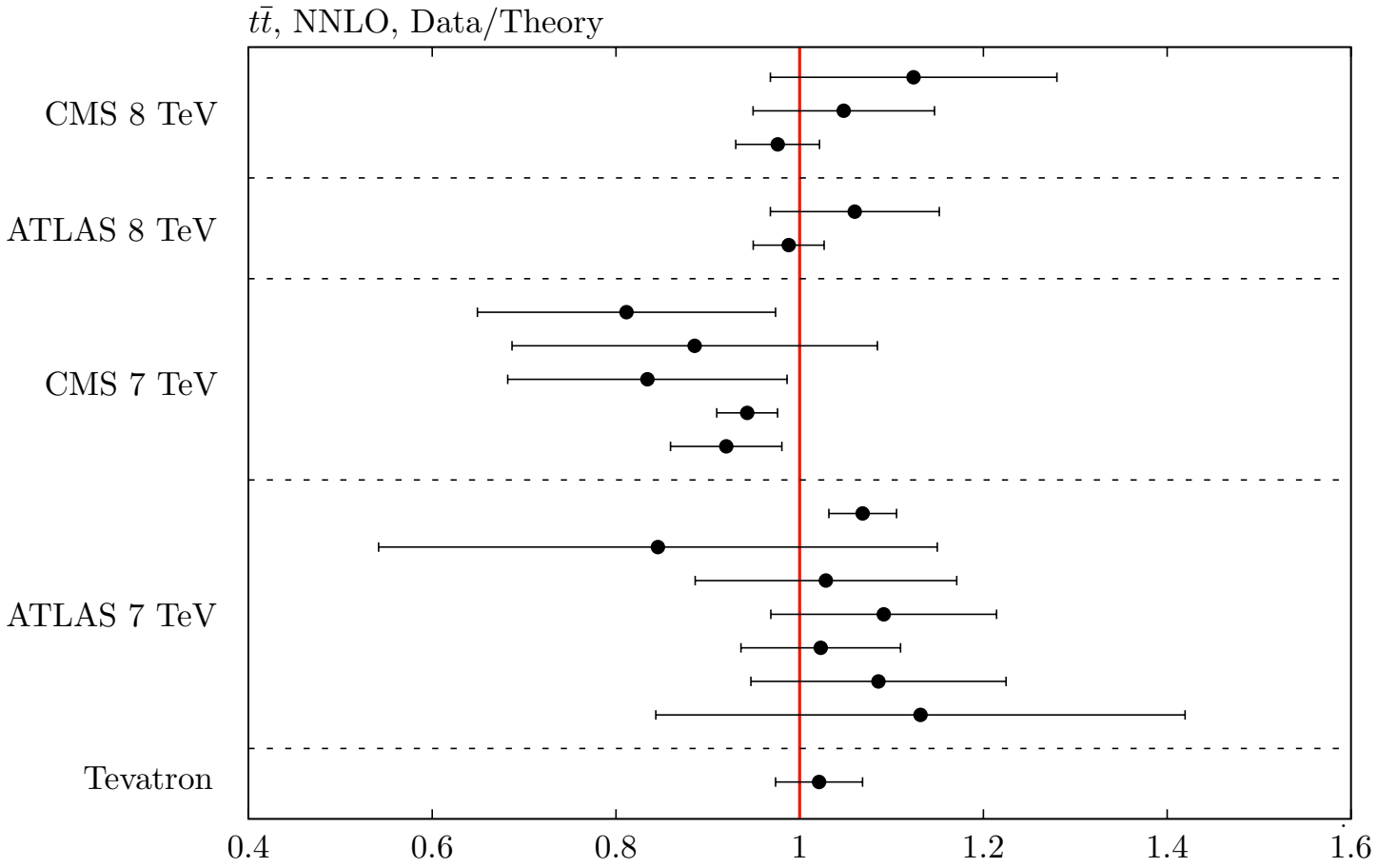

Fit very good and with $\alpha_S(M_Z^2) = 0.118$ the fitted $m_t^{pole} = 173.4$ GeV. At NLO $m_t^{pole} = 170.2$ GeV. MMHT values $m_t^{pole} = 174.2$ GeV and $m_t^{pole} = 171.7$ GeV

Helps drive slight increase in $\alpha_S(M_Z^2)$

Inclusion of high precision ATLAS W, Z data arXiv:1612.03016

For MMHT PDFs with final HERA combined data (and some more $\sigma_{t\bar{t}}$ points) obtain $\chi^2/N_{pts} \sim 387/61$. Use this as our "baseline".

Including ATLAS W, Z data in fit goes to $\chi^2/N_{pts} \sim 130/61$, similar to ATLAS profiling. Use this as basis for study of effects on PDFs.

Deterioration in fit to other data $\Delta\chi^2 = 54$. Worst for CMS double differential Z/γ data ($\Delta\chi^2 = 17$) and CCFR/NuTeV dimuon data ($\Delta\chi^2 = 16$). For latter branching ratio requires 25% shift.

Other deterioration in fixed target DIS data, E866 Drell-Yan asymmetry and CDF W-asymmetry.

Also try fit with scales set to $\mu_{R,F} = M_{W,Z}/2$ rather than $\mu_{R,F} = M_{W,Z}$ (thanks to V. Radescu, A. Cooper-Sarkar)

As in ATLAS study find reduction in χ^2 of about 20 units, i.e. to $\chi^2/N_{pts} \sim 106/61$ - relatively spread over different data sets.

Almost no change in fit to other data.

Prediction and Fit to data

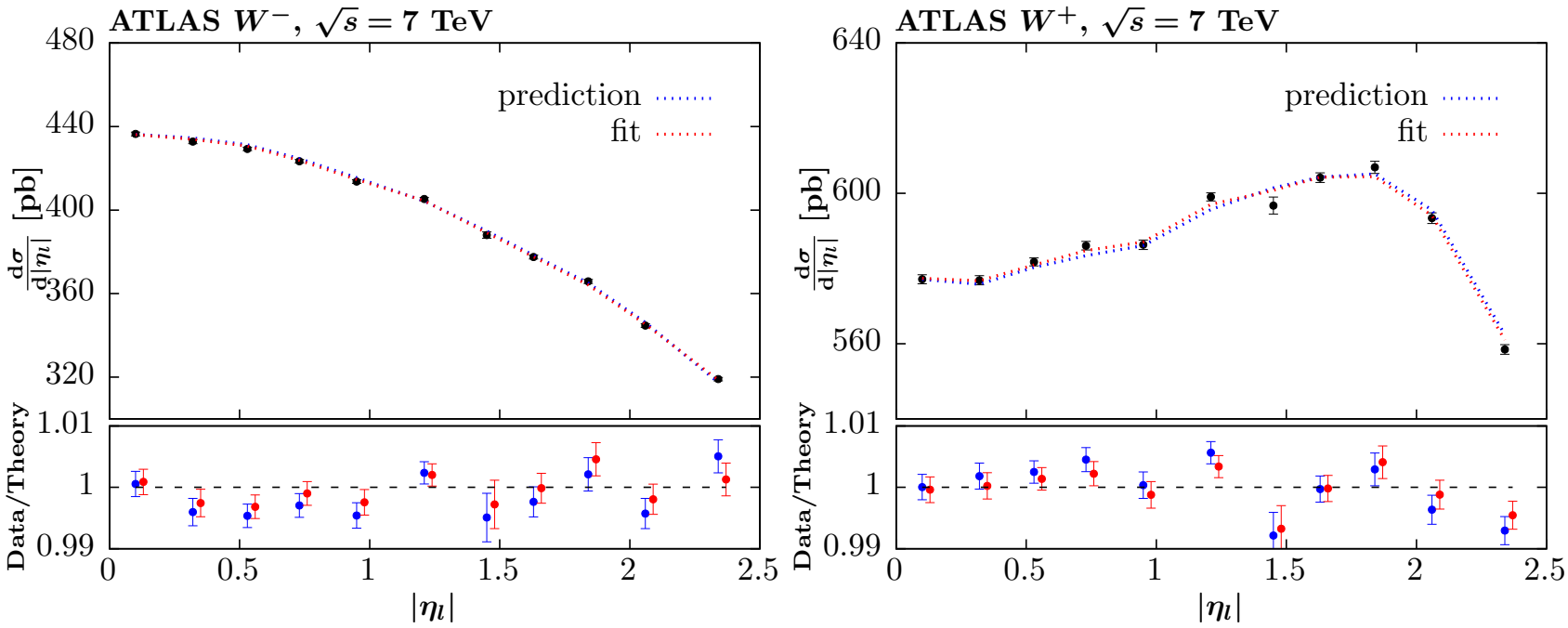

Slight reduction in lower $|\eta|$ W^- required and opposite for W^+.

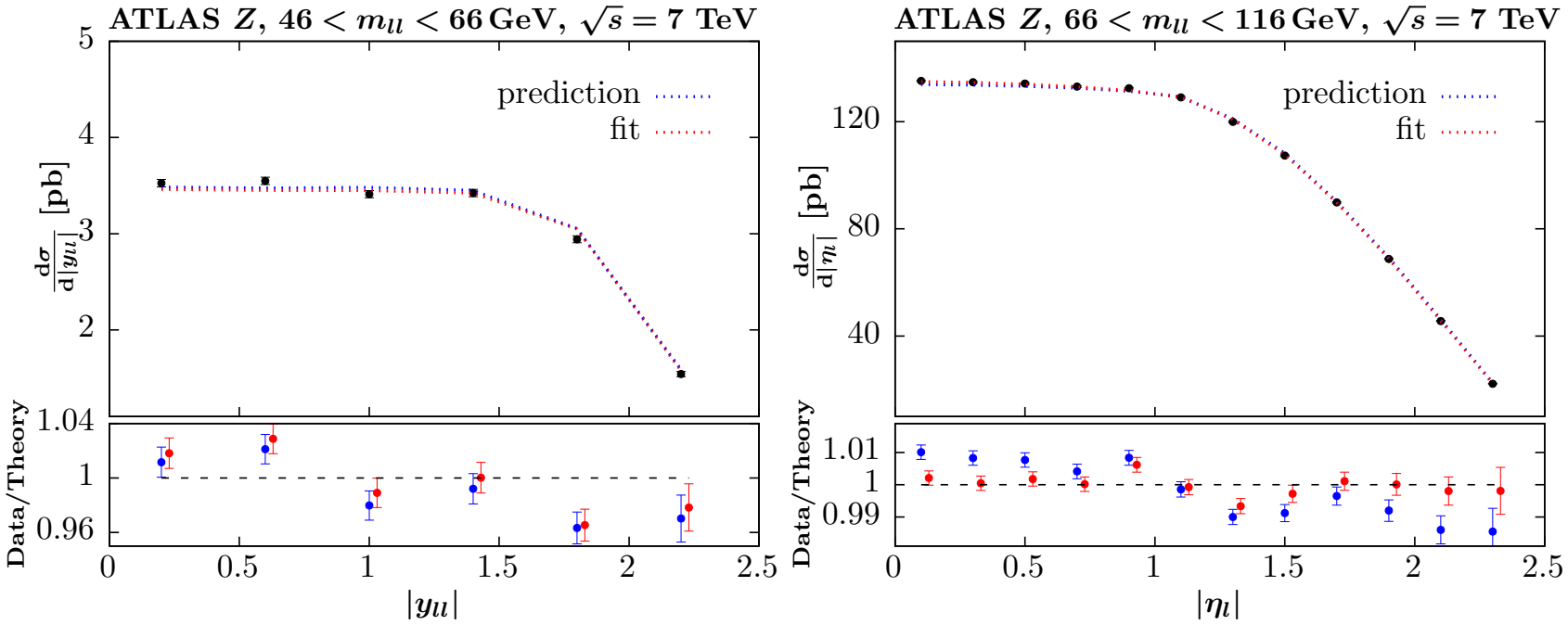

Significant change in shape required for Z production, Higher at low $|\eta|$ and lower at high $|\eta|$

Even with fit difficulty in shape for lower mass data.

Fully Updated Fit with all new LHC data

Also perform fit where all other new LHC data from LHCb and CMS included. Compared to baseline plus ATLAS W, Z data very little change.

However, inclusion of ATLAS W, Z data lowers χ^2 for new LHC (plus final D0) data by $\Delta\chi^2 = -10$.

Hence ATLAS W, Z data and other new LHC data compatible and pull in same direction. Only CMS $W + c$ deteriorates slightly.

Generate PDF eigenvector sets for uncertainties at NNLO using same basis of 25 free PDF parameters as in MMHT2014 (this is subject to possible/likely change in the future).

Hence, 50 eigenvector directions.

21 of these are best constrained by one of the new (LHC) data sets.

Effect on PDFs

Large increase in $s + \bar{s}$ and decrease in uncertainty. Correlation with fit to dimuon data (lower branching ratio) leads to increase at high x.

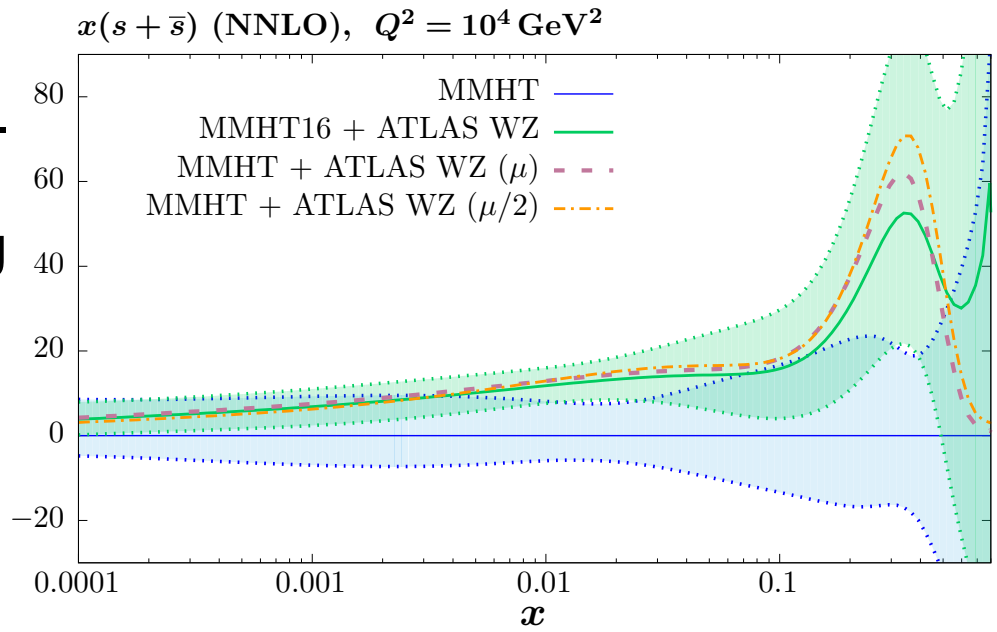

Larger for $x > 0.1$ due to significant down quark contribution in this region despite Cabibbo suppression.

There is impact on $s - \bar{s}$ uncertainty, from the change in branching ratio.

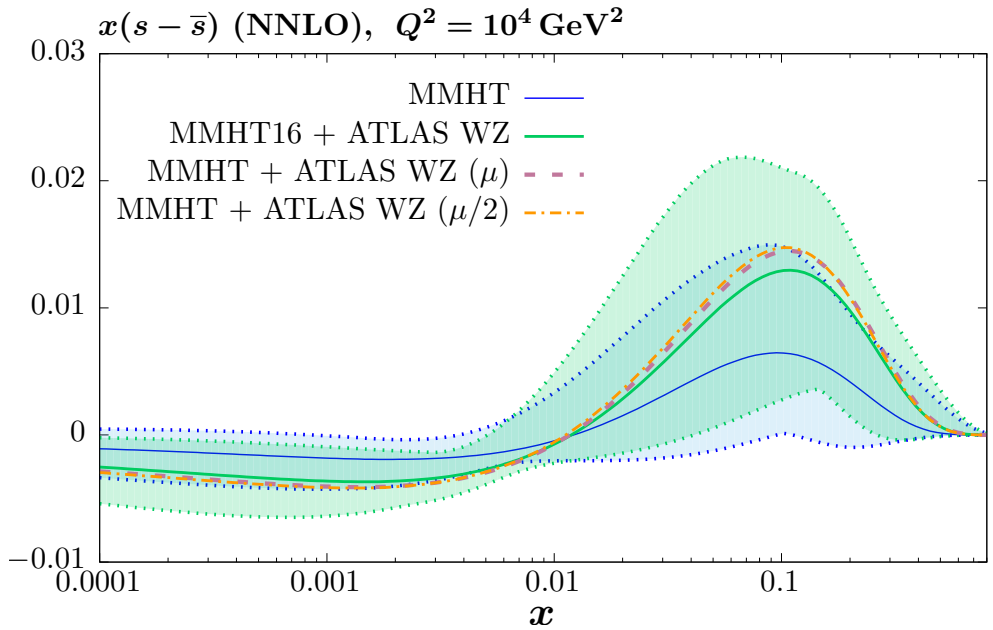

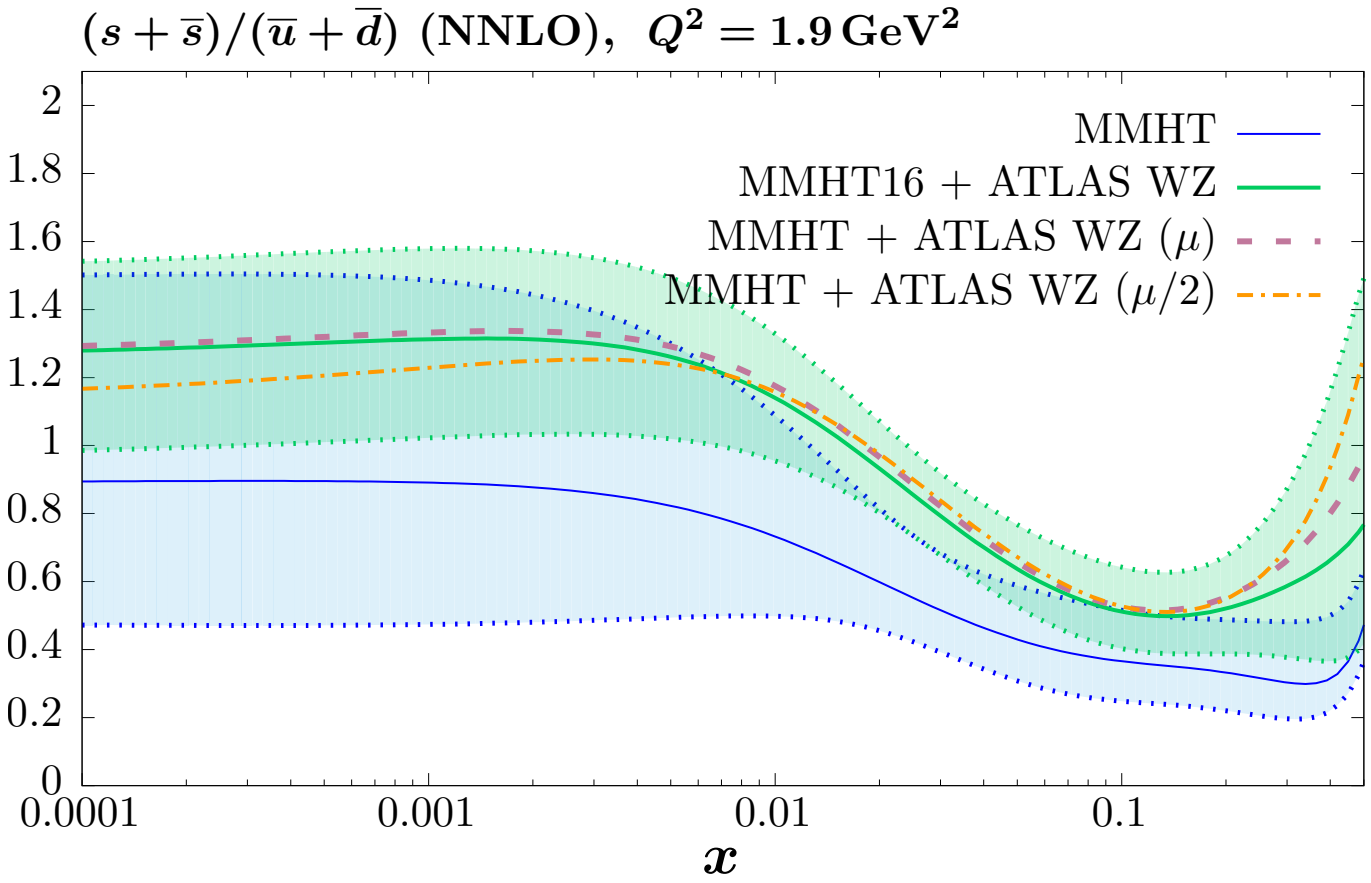

Ratio of $(s+\bar{s})$ to $\bar{u}+\bar{d}$, i.e. R_s at $Q^2 = 1.9\ \mathrm{GeV}^2$.

At $x = 0.023$ $R_s \sim 0.83 \pm 0.15$. Compare to ATLAS with $R_s = 1.13^{+0.08}_{-0.13}$

R_s exceeds unity at lower x, but essentially an extrapolation. Comfortably consistent with unity.

Significant impact on shape of valence quarks.

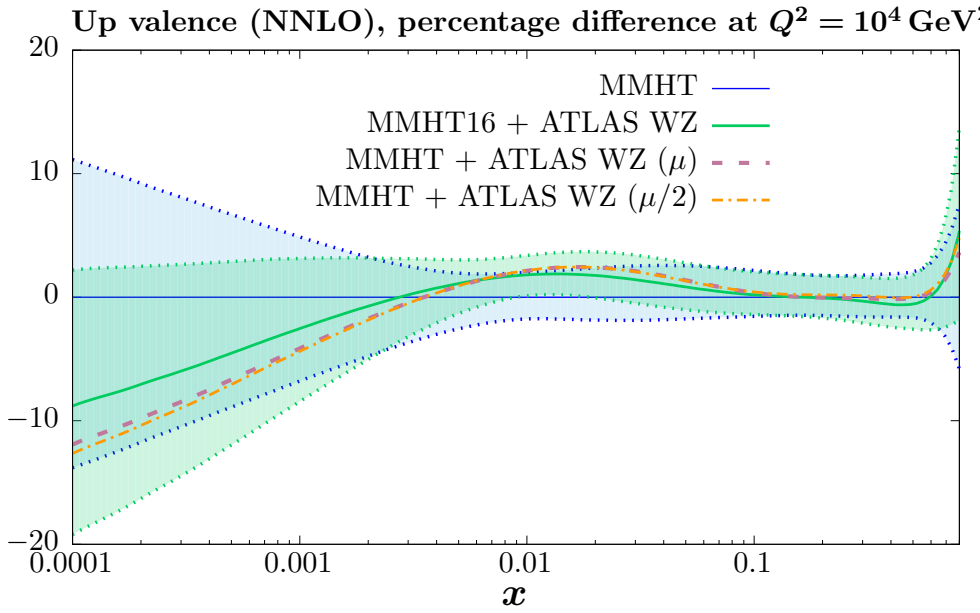

Same direction as impact of other new LHC data.

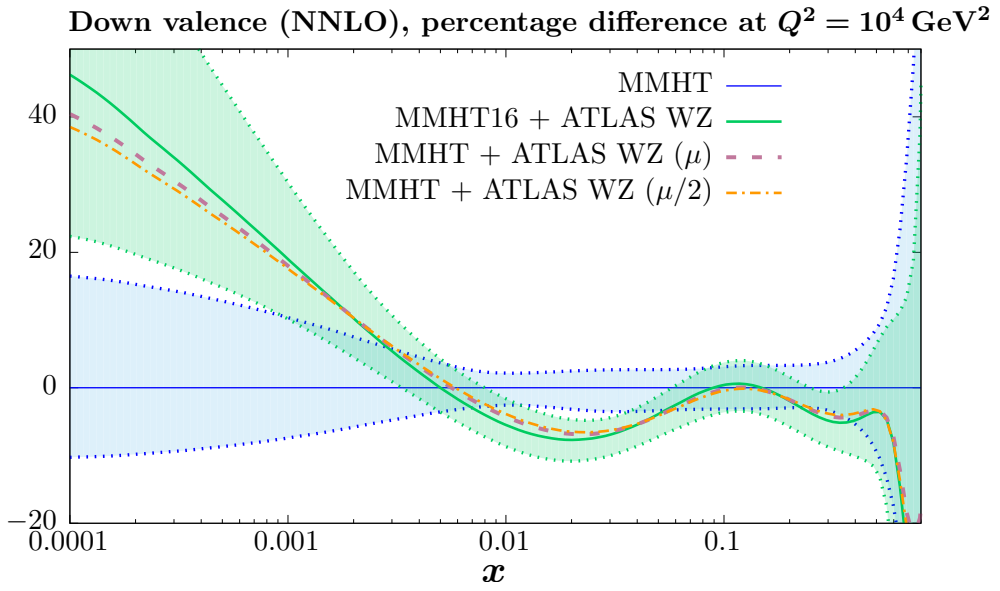

PDFs with QED corrections

At the level of accuracy we are now approaching it is important to account for electroweak corrections. At the LHC this can be important for many processes ($W, Z, WH, ZH, WW, jets \ldots$).

For a consistent treatment need PDFS which incorporate QED into the evolution, i.e. the inclusion of the photon PDF $\gamma(x, Q^2)$.

(A. De Rujula *et. al.* NPB154 (1979) 394, J. Kripfganz and H. Perlt, ZPC41 (1988) 319, J. Blümlein, ZPC47 (1990) 89.)

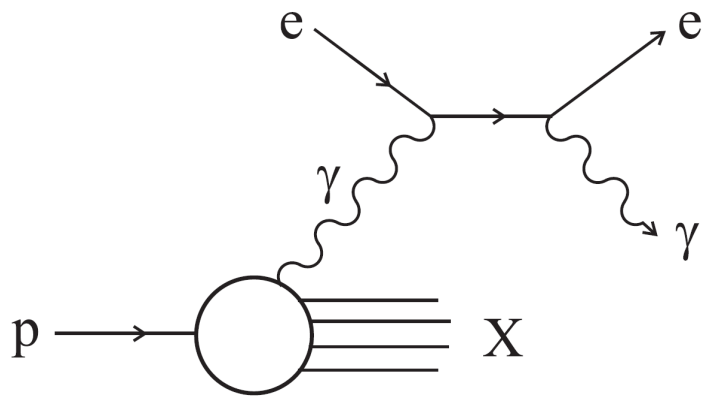

$$\frac{\partial\gamma(x,Q^2)}{\partial \log Q^2} = \frac{\alpha}{2\pi}\int_x^1 \frac{dy}{y}\left(P_{\gamma\gamma}\otimes\gamma + \sum_1 e_i^2 P_{\gamma q}\otimes q_i\right)$$

Set published by NNPDF and recently CT.

MRST2004 assumed $\gamma(x, Q^2)$ generated by photon emission off model for valence quarks with QED evolution from $m_q \rightarrow Q_0^2$. Freedom in choice of quark mass, e.g. current mass $\rightarrow$ constituent mass.

Various articles (M. Gluck et al., PLB, 540,75 (2002), A.D. Martin and M.G. Ryskin, EPJ C74, 3040 (2014) considers separate "coherent" emission and "non-coherent" emission.

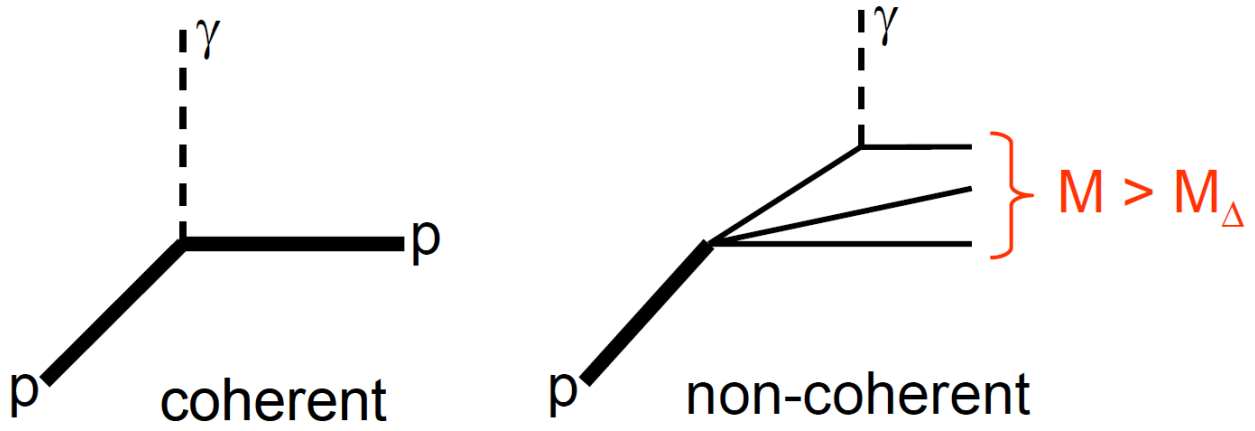

$$\gamma^N(x, Q_0^2) = \gamma^N_{\rm coh} + \gamma^N_{\rm incoh}$$

Breakdown into well-known elastic (coherent) contribution and moderately model dependent inelastic part Harland-Lang *et al*. PRD94 (2016) 074008. Much better constraint on input.

Put on truly quantitative footing in LUXqed photon PDF (A. Manohar et al., PRL 117, 242002 (2016), arXiv:1708.01256).

LUXqed

- Recent study of arXiv:1607.04266:

CERN-TH/2016-155

How bright is the proton?
A precise determination of the photon PDF

Aneesh Manohar,[1,2] Paolo Nason,[3] Gavin P. Salam,[2,*] and Giulia Zanderighi[2,4]
[1] *Department of Physics, University of California at San Diego, La Jolla, CA 92093, USA*
[2] *CERN, Theoretical Physics Department, CH-1211 Geneva 23, Switzerland*
[3] *INFN, Sezione di Milano Bicocca, 20126 Milan, Italy*
[4] *Rudolf Peierls Centre for Theoretical Physics, 1 Keble Road, University of Oxford, UK*

- Show how photon PDF can be expressed in terms of F_2 and F_L. Use measurements of these to provide well constrained LUXqed photon PDF.

$$x f_{\gamma/p}(x,\mu^2) = \frac{1}{2\pi\alpha(\mu^2)}\int_x^1 \frac{dz}{z}\left\{ \int_{\frac{x^2 m_p^2}{1-z}}^{\frac{\mu^2}{1-z}} \frac{dQ^2}{Q^2}\alpha^2(Q^2) \right.$$
$$\left[\left(z p_{\gamma q}(z) + \frac{2x^2 m_p^2}{Q^2}\right) F_2(x/z, Q^2) - z^2 F_L\left(\frac{x}{z}, Q^2\right)\right]$$
$$\left. - \alpha^2(\mu^2) z^2 F_2\left(\frac{x}{z}, \mu^2\right)\right\}, \quad (6)$$

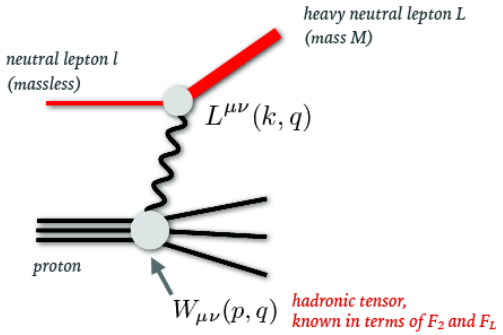

22

Relates photon to structure functions, and hence precision of at worst a few percent.

MMHT PDFs with QED corrections – Nathvani

We now base photon input for PDFs at low Q^2 on the LUXqed prescription, MMHT photon (Nathvani) very similar to LUXqed.

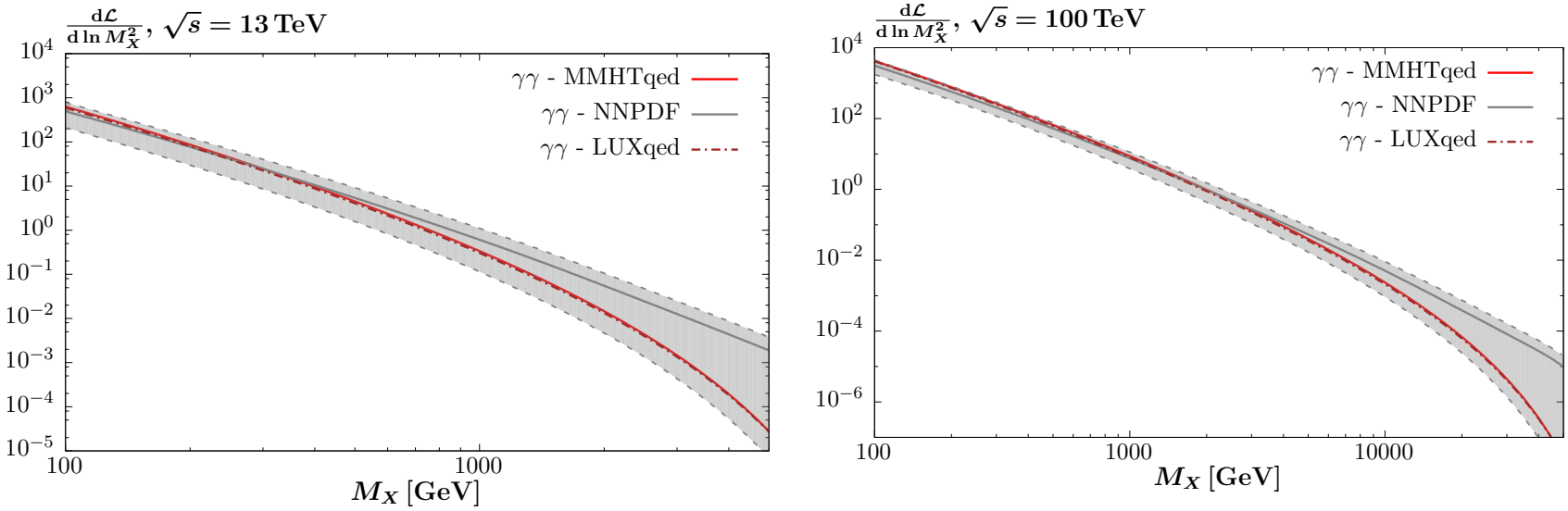

Effect of photon evolution fully incorporated to couple with that of quarks and gluon for both proton and neutron.

Evolution now included at $\mathcal{O}(\alpha + \alpha_S\alpha + \alpha^2)$.

Details of Photon distribution

The photon input is defined at $Q_0^2 = 1\mathrm{GeV}^2$, the same as other PDFs.

Input defined by integrating LUX expression up to scale $\mu^2 = Q_0^2$. Hence contribution up to this scale should be identical. (Minor difference from using μ^2 rather than $\mu^2/(1-z)$ as integral limit, with correction in last term $\propto \ln(1-z)P_{\gamma q}$.)

Above this all PDFs evolve according to DGLAP evolution up to given order in α_s with all order $\alpha, \alpha\alpha_S$ and α^2 correction to splitting functions included.

In addition the photon receives contributions from coherent scattering and terms $\propto x^2/Q^2$ in quark-photon splitting function. Important for high x.

In principle both contributions higher twist and violate momentum conservation in evolution. In practice former generates momentum 4.75×10^{-5} and latter about a third of this. Therefore negligible in practice.

Significant relative effect to high-x photon, but absolute magnitude tiny.

Corrections beyond $\mathcal{O}(\alpha)$.

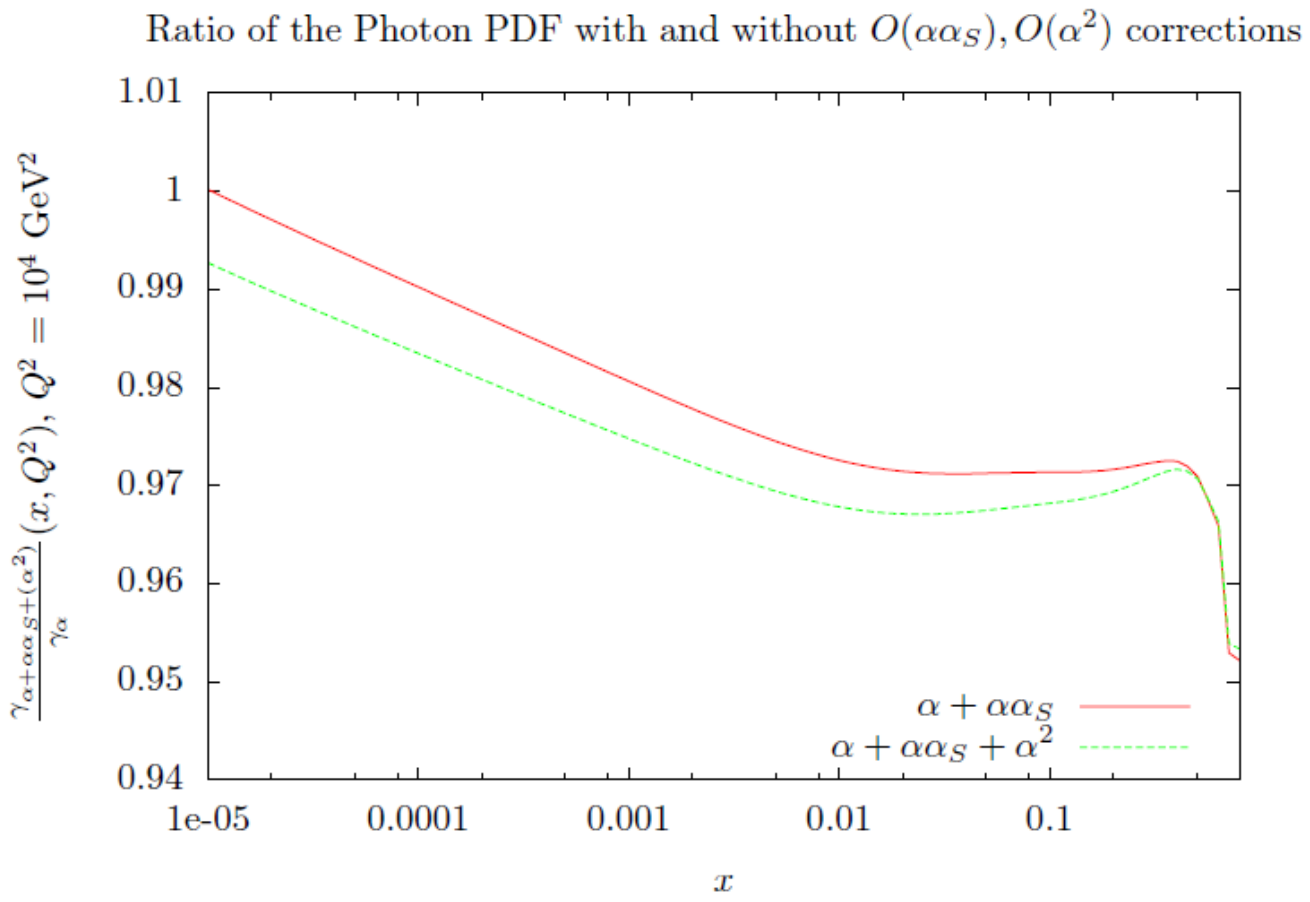

Corrections negative and larger at high x.

Corrections from coherent contribution and higher twist above input

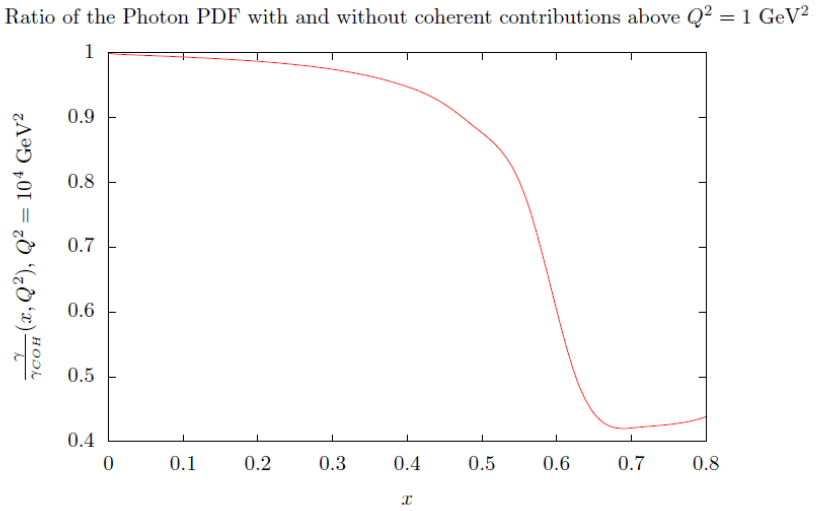

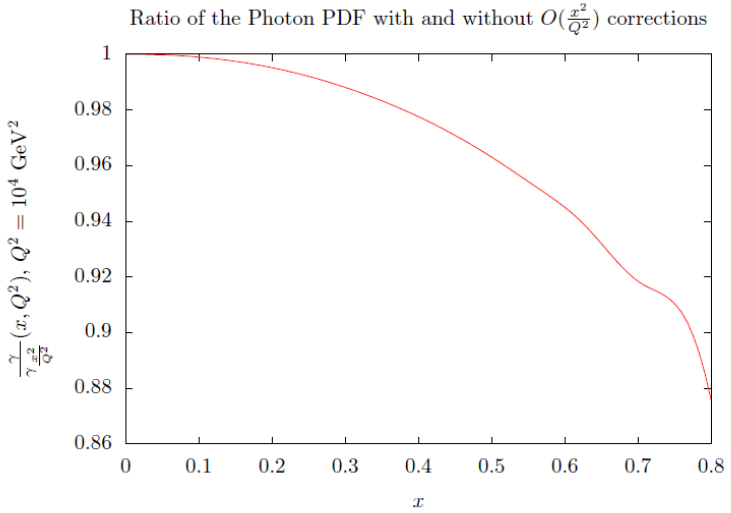

Coherent contributions above input very significant at very high x.

x^2/Q^2 correction significant.

Both only where the photon is tiny though. Very small effect on PDF momentum.

Photon-Photon Luminosity

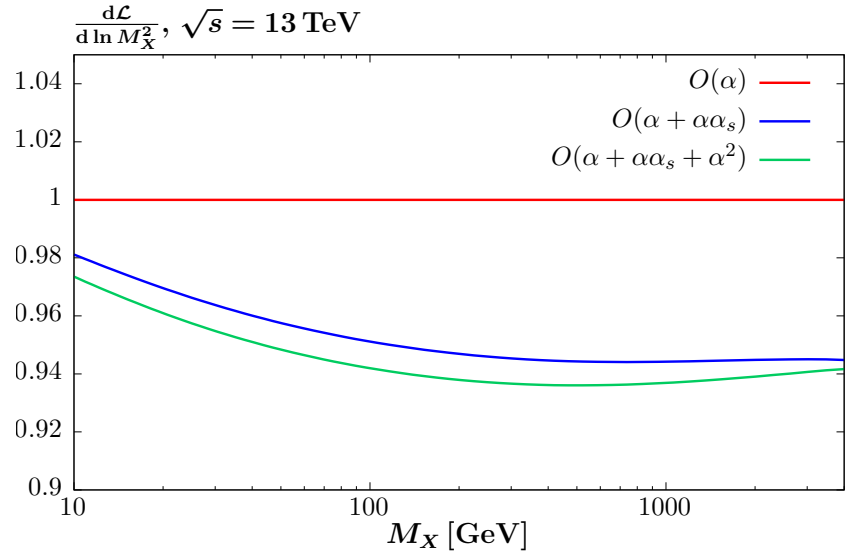

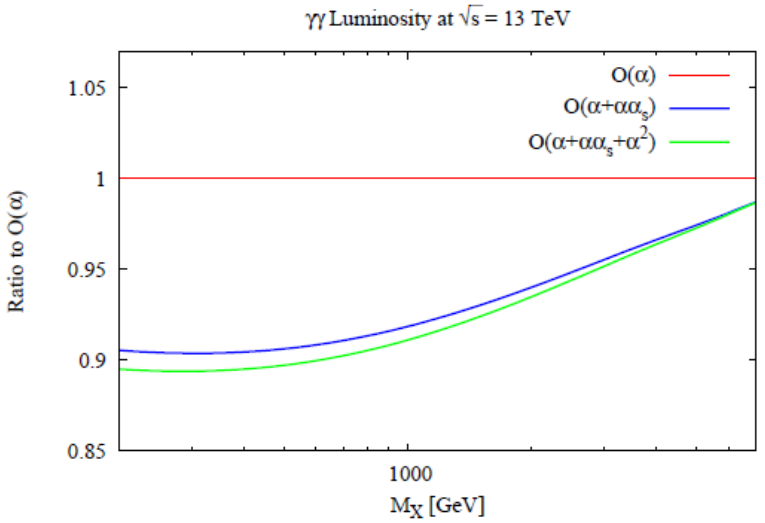

Smaller effect than for NNPDF3.0 photon (right), F. Giuli, *et al*, EPJC77 (2017) 400.

(Note different scale on horizontal axes.)

Comparison to LUXqed photon.

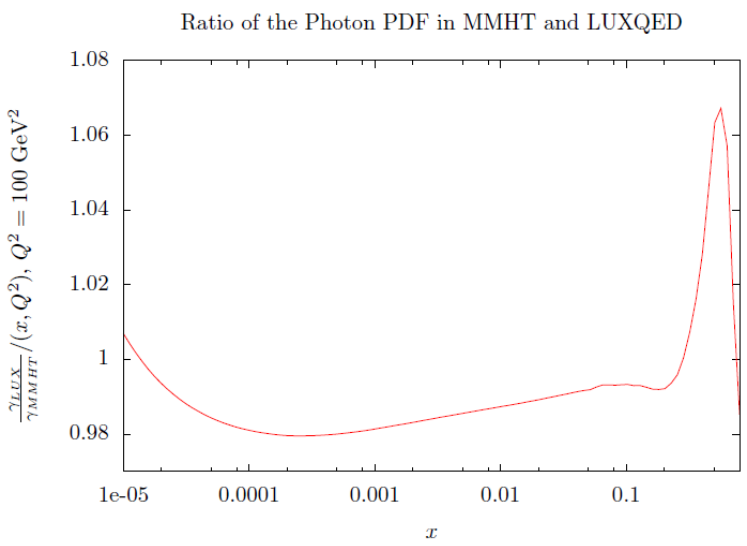

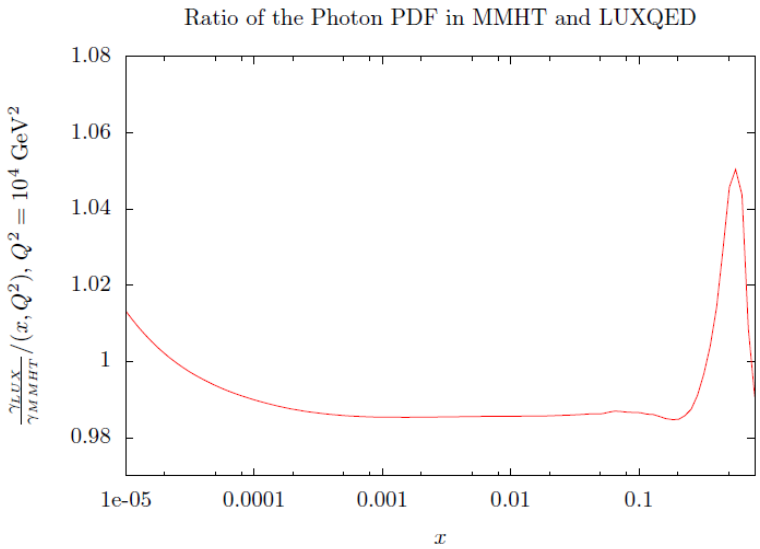

Only significant difference at very high x where uncertainties getting large .

Change from QCD order

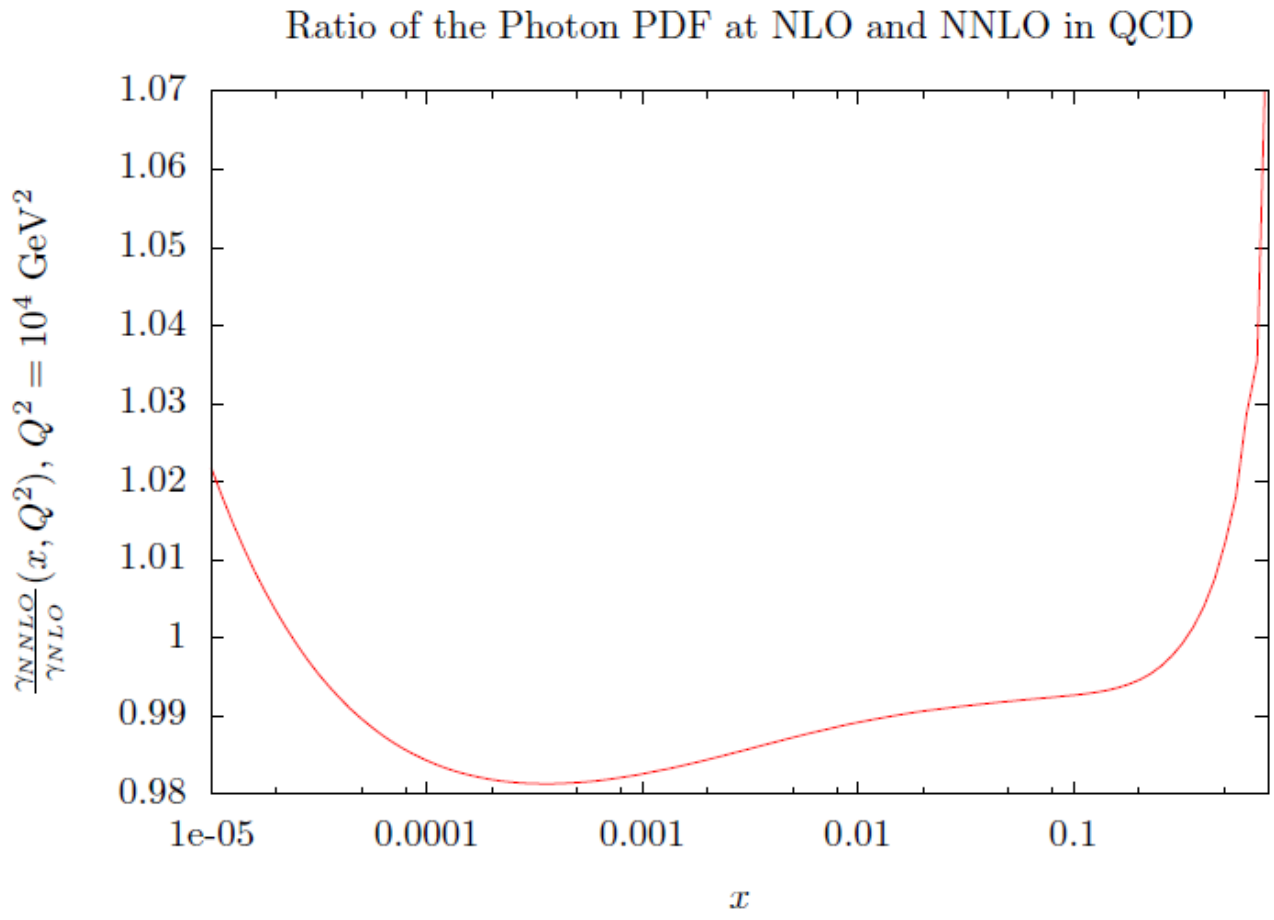

Reflects differences in quarks between orders.

Difference to LUXqed.

MMHT14 quarks slightly less hard at high x than PDF4LHC at level of one sigma.

Evolution in LUXqed contains some higher order terms

$$\frac{d\,x f_{\gamma/p}(x,\mu^2)}{d\,\ln\mu^2} = \frac{\alpha(\mu^2)}{2\pi}\int_x^1 \left\{ \left[\left(zP_{\gamma q}(z) + \frac{2z^2 m_p^2}{\mu^2} \right) F_2(x/z,\mu^2) \right. \right.$$
$$\left. \left. -z^2 F_L(x/z,\mu^2) \right] - z^2 \frac{d\,F_2(x/z,\mu^2)}{d\,\ln\mu^2} \right\}.$$

If $F_2(x/z,\mu^2)$ is the NNLO expression then the first term contains parts $\propto \alpha\alpha_S^2 P_{\gamma q} \otimes C_{2q}^2 \otimes q$ and last term contains parts $\propto \alpha\alpha_S^2 P_{qf}^1 \otimes f$ and other higher orders, e.g. $\propto \alpha\alpha_S^2\beta_0 C_{2q}^1 \otimes q$. The first and last are enhanced at large x.

we use only the perturbative leading twist expression for $F_2(x/z,\mu^2)$ above input, even at high x where W^2 is small.

Inputs for the Neutron

For the coherent part the form factors for the neutron are used. The data is not very precise and gives a very small contribution.

For the incoherent part the neutron approximation is achieved by assuming that the ratio of the structure functions is well approximated by the ratio of partons at input between the neutron and protons

$$rF_2(Q_0^2) = \frac{4(d(Q_0^2) + \bar{d}(Q_0^2)) + (u(Q_0^2) + \bar{u}(Q_0^2)) + (s(Q_0^2) + \bar{s}(Q_0^2))}{4(u(Q_0^2) + \bar{u}(Q_0^2)) + (d(Q_0^2) + \bar{d}(Q_0^2)) + (s(Q_0^2) + \bar{s}(Q_0^2))}$$

Consequently the neutron input photon carries less momentum than for the proton. This must be reflected in other PDFs.

$$\int_0^1 dx\, x(\gamma^p - \gamma^n) \approx 0.0015$$

No reason to assume this is manifest in the gluon – more suitable in valence quarks where radiation of photon depends on charge.

Photon in Neutron

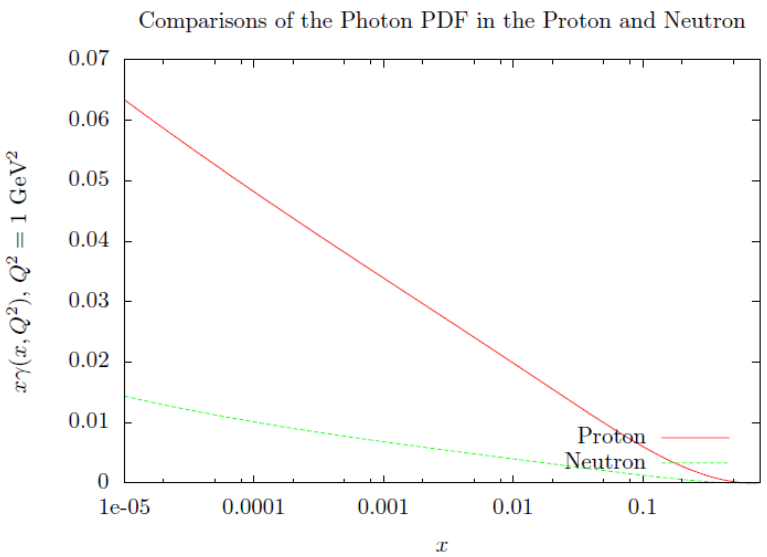

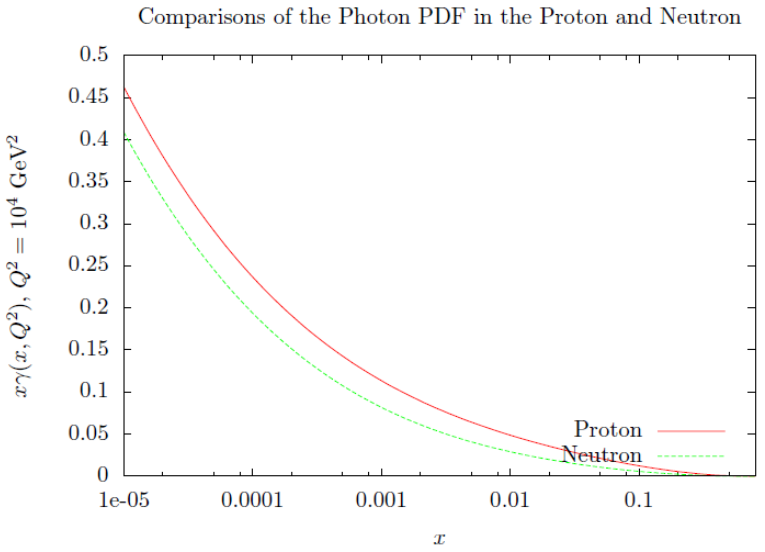

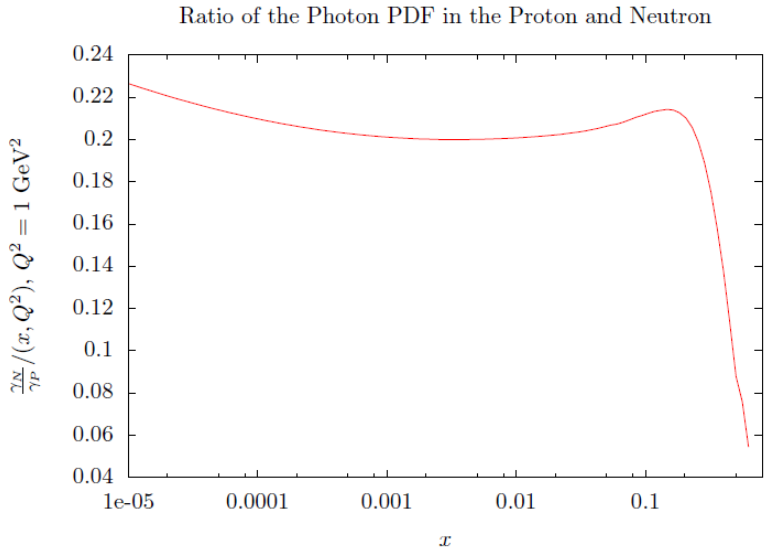

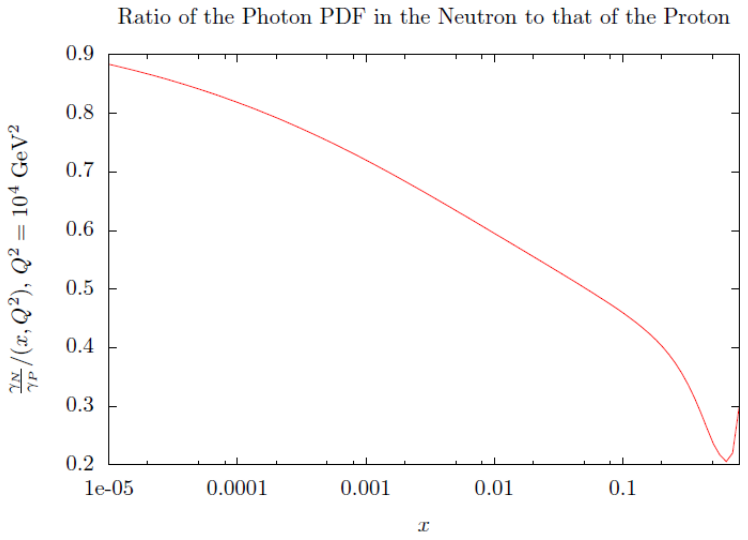

Differences at small x wash out at higher Q^2.

An isospin violating component of the neutron $\Delta d_V^n = d_V^n - u_V^p$ comes in during evolution.

MRST introduced an isospin-violating component at input (whose zeroth moment vanishes to obey sum rules) was determined by the difference between u_V^p and d_V^p, with the constant of proportionality being determined by conservation of momentum.

We now assume that the difference introduced is proportional to the contribution to valence distributions from QED evolution.

$$\Delta d_V^n = \epsilon(1 - \frac{e_d^2}{e_u^2})\Delta u_V^{QED}; \qquad \Delta u_V^n = \epsilon(1 - \frac{e_u^2}{e_d^2})\Delta d_V^{QED}$$

taken from the integration step immediately after input.

The constant of proportionality is then set by conservation of momentum, similar to MRST.

$$\epsilon = \frac{\int_0^1 dx\, x(\gamma^p - \gamma^n)}{\int_0^1 dx\, x(3/4\Delta u_V^{QED} - 3\Delta d_V^{QED})}$$

Isospin violating changes in valence quarks in Neutron

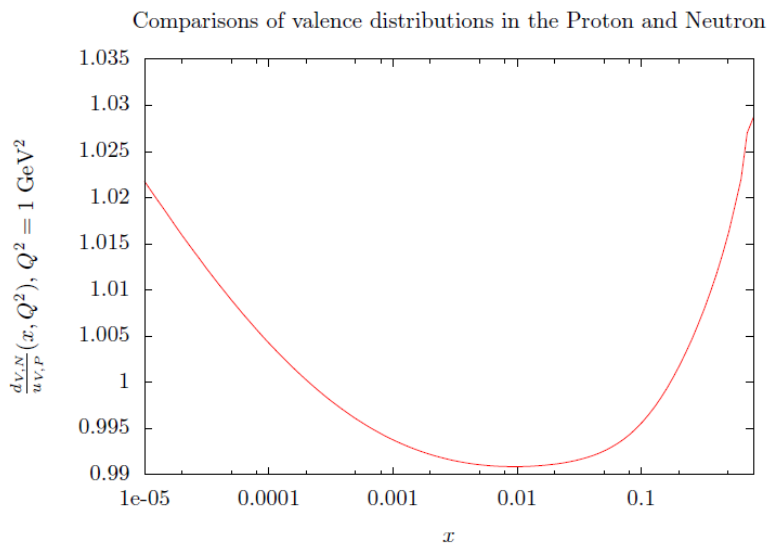

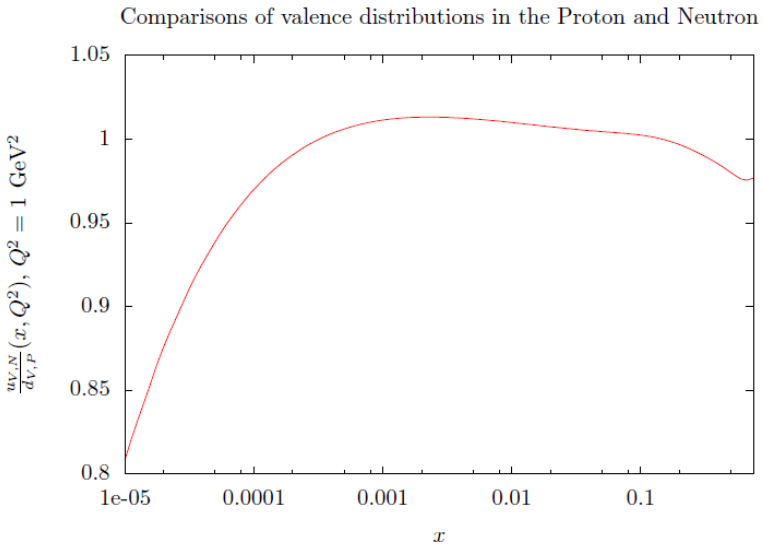

Differences reflect respective QED evolution.

QED corrected PDF fit

As well as correcting evolution, corrections to DIS coefficient functions at $\mathcal{O}(\alpha)$ added.

At NLO $\Delta\chi^2 = 28$ before refit $\rightarrow$ $\Delta\chi^2 = 17$ after refit.

At NNLO $\Delta\chi^2 = 29$ before refit $\rightarrow$ $\Delta\chi^2 = 13$ after refit.

Increased evolution speed of quarks at high x leads to $\Delta\chi^2 = 5$ for BCDMS data.

At NLO some effect in NMC and HERA CC data as well.

At NNLO no significant change in any other data set.

Change in PDFs due to refit

Large x u_V increased at input since loss greater due to extra photon radiation. $\rightarrow$ larger d_V in neutron.

d_V hardly changes at input (less photon radiation). In fact marginally less momentum.

Sea quarks carry slightly more momentum.

Loss of gluon momentum in QED corrected PDFs after refit > 1.5 times more than input momentum carried by photon.

QED effect on other partons

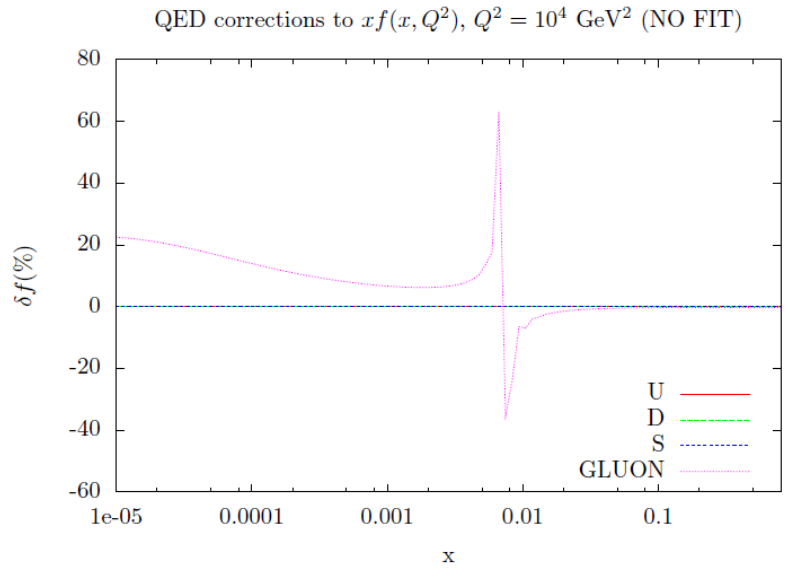

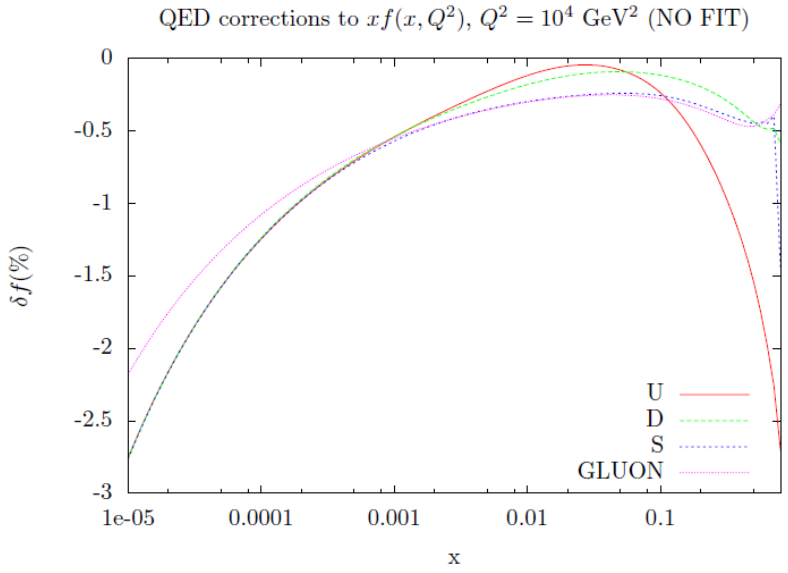

At input the inclusion of the photon is all taken account of in the gluon since a gluon parameter is fixed from the momentum sum rule. Affects small x.

Quarks decrease with evolution at high x due to photon radiation.

All PDFs decrease at small x due to smaller input gluon.

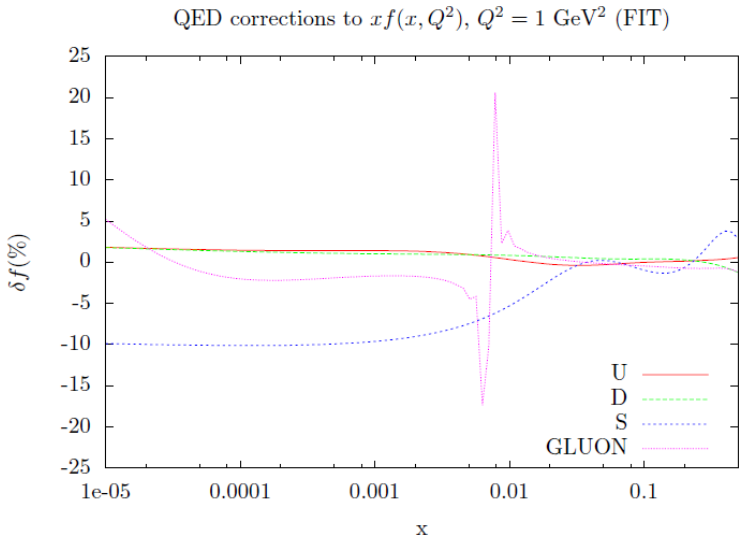

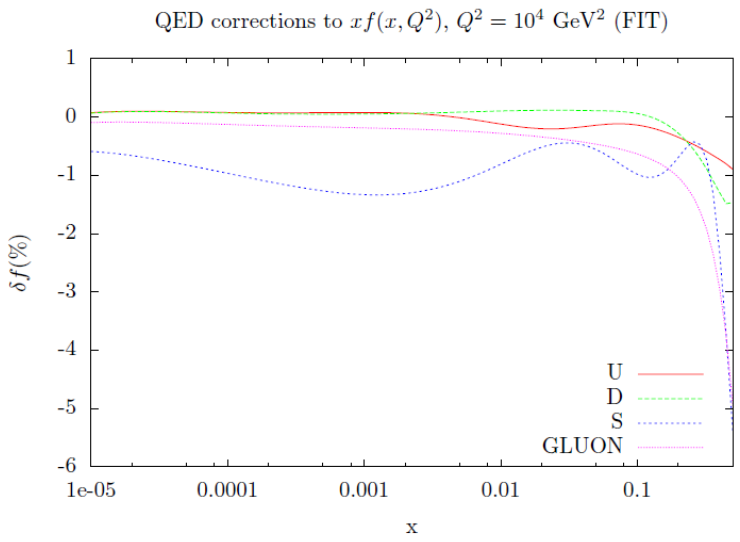

Differences induced by QED altered significantly in refit.

Gluon affected more widely over x, less at small x.

Small x flavour rearrangement in quarks – less strange.

Quarks lose momentum at high x from QED evolution, but reduction in high Q^2 up quark less as compensated for by input.

Effect of refit on photon

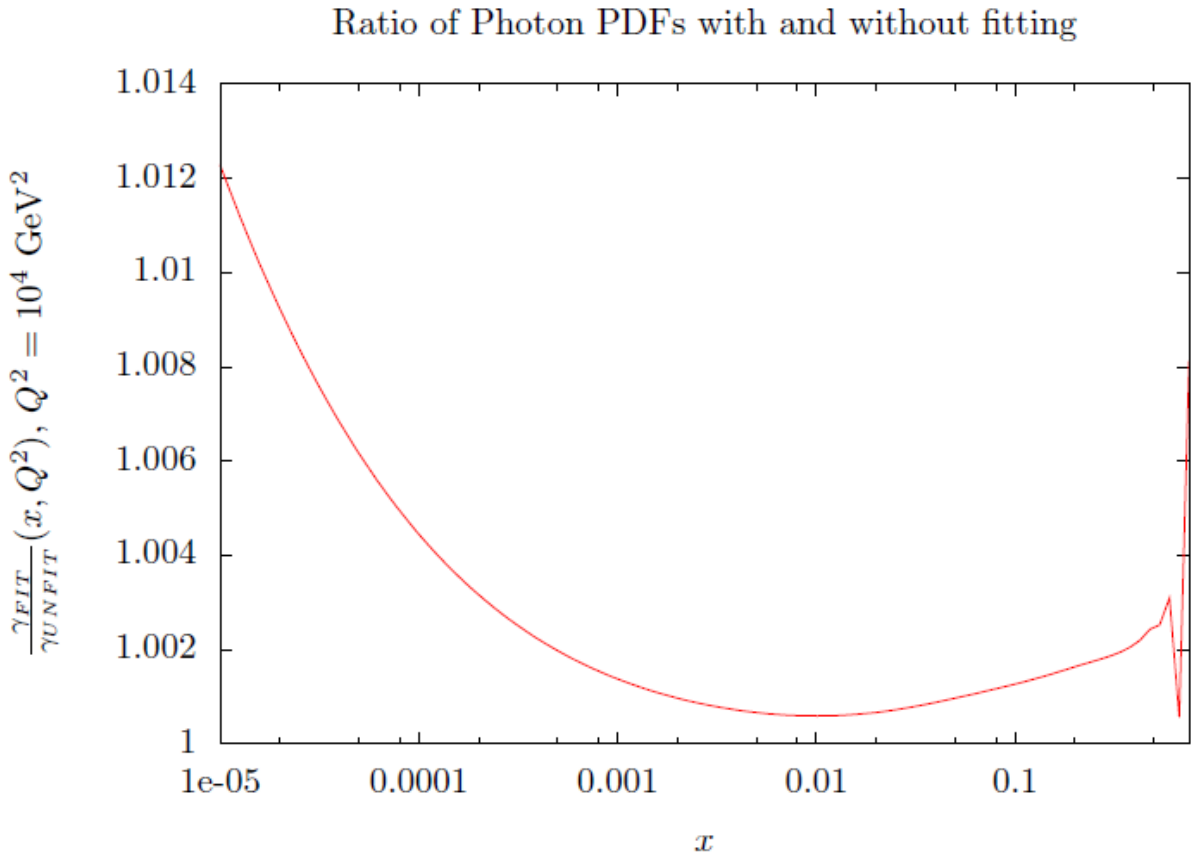

Tiny increase mainly due to larger up quark contribution.

Conclusions

MMHT partons predict most recent vector boson production data (and top quark pair cross section data well). Most recent high precision ATLAS 7 TeV W,Z data an exception for real quantitative fit.

Refits good, but ATLAS data in tension with older CMS Drell Yan data and with fixed target dimuon data (latter awaiting full NNLO corrections). All included recent data very consistent among themselves.

Increase in strange quark fraction and in low $x\, u_V - d_V$.

First results on new QED corrected partons with the photon input at $Q_0^2 = 1\ \mathrm{GeV}^2$ given by LUXqed.

"Higher twist" contributions above Q_0^2 significant, but not for sum rule.

Some small differences in photon compared to LUXqed.

Refit PDFs different in detail to those where photon and QED evolution just added to fixed input PDFs.

Neutron PDFs obtained with some assumptions/approximations for inputs of photon and quarks consistent with sum rules.

Back-up

Change scales to $\mu_{R,F} = M_{W,Z}/2$

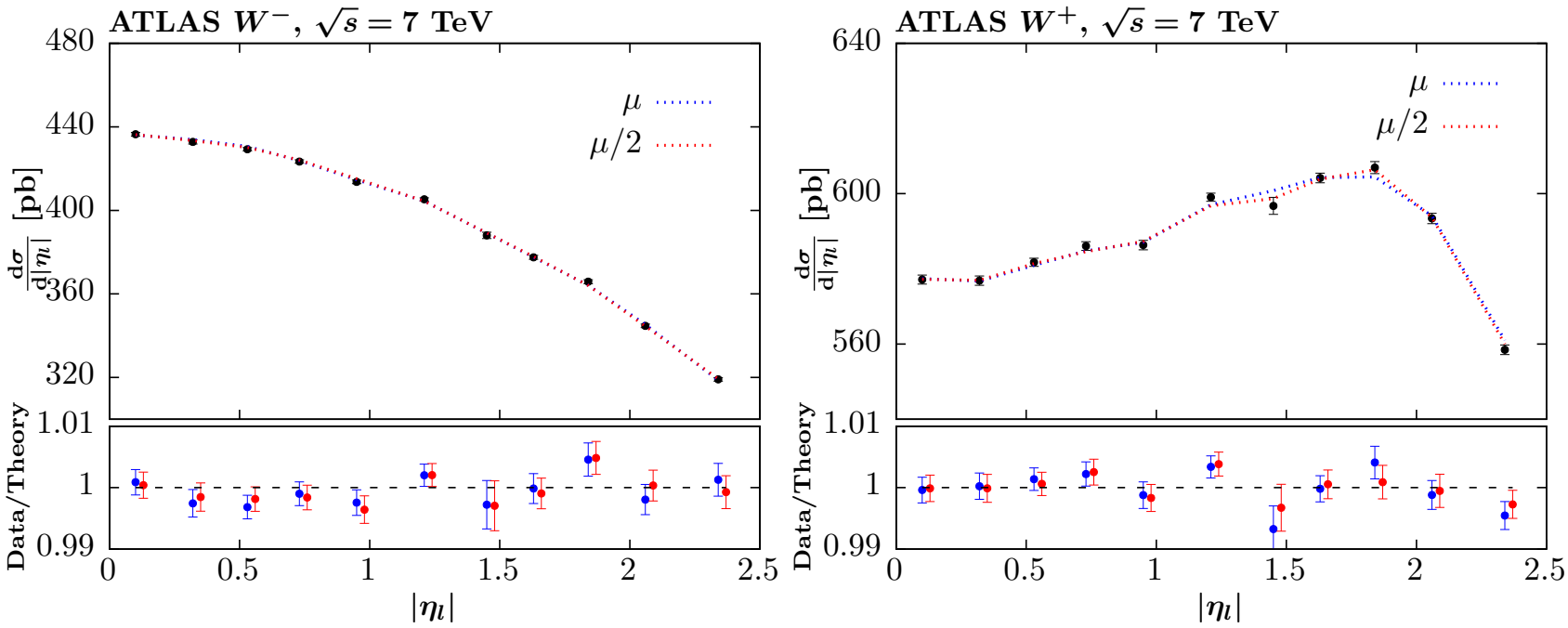

More noticeable improvement for W^+.

As implied by individual distributions, significant change in $u_V - d_V$.

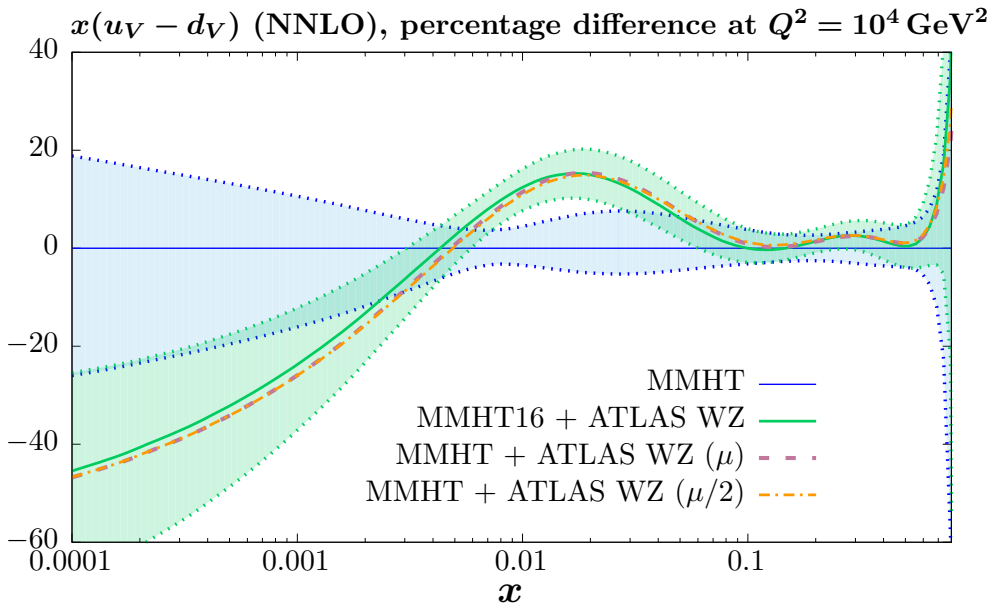

Shift in best fit $\bar{d} - \bar{u}$ accompanying deterioration in fit to E866 Drell-Yan asymmetry.

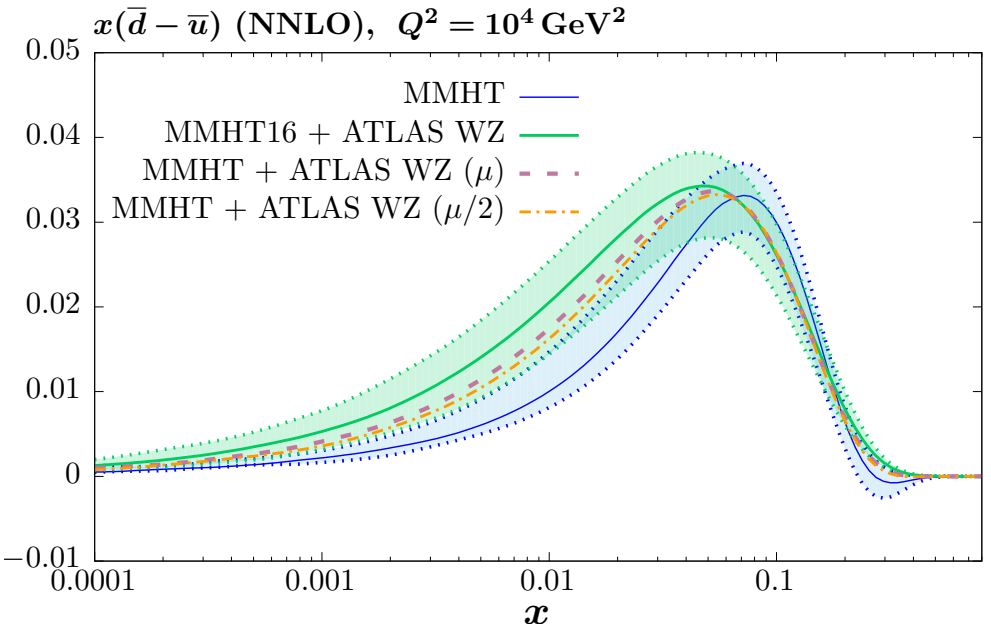

Extension of $\bar{d} - \bar{u}$ parameterisation.

Currently use 3 free parameters, i.e.

$$(\bar{d} - \bar{u})(x, Q_0^2) = A(1-x)^{\eta_{sea}+2} x^{\delta}(1 + \gamma x + \Delta x^2),$$

Extend to

$$(\bar{d} - \bar{u})(x, Q_0^2) = A(1-x)^{\eta_{sea}+2} x^{\delta}(1 + \sum_{i=1}^{4} a_i T_i(1 - 2x^{\frac{1}{2}})),$$

where $T_i(1 - 2x^{\frac{1}{2}}))$ are Chebyshev polynomials. So 5 free parameters. Easily allows multiple turning points (seen in first fit iteration).

Global fit including new LHC data and new ATLAS W, Z data improves by 10 units, but over 5 of this in E866 Drell Yan asymmetry.

Parameterisation alleviates some tension between ATLAS data and Drell Yan asymmetry.

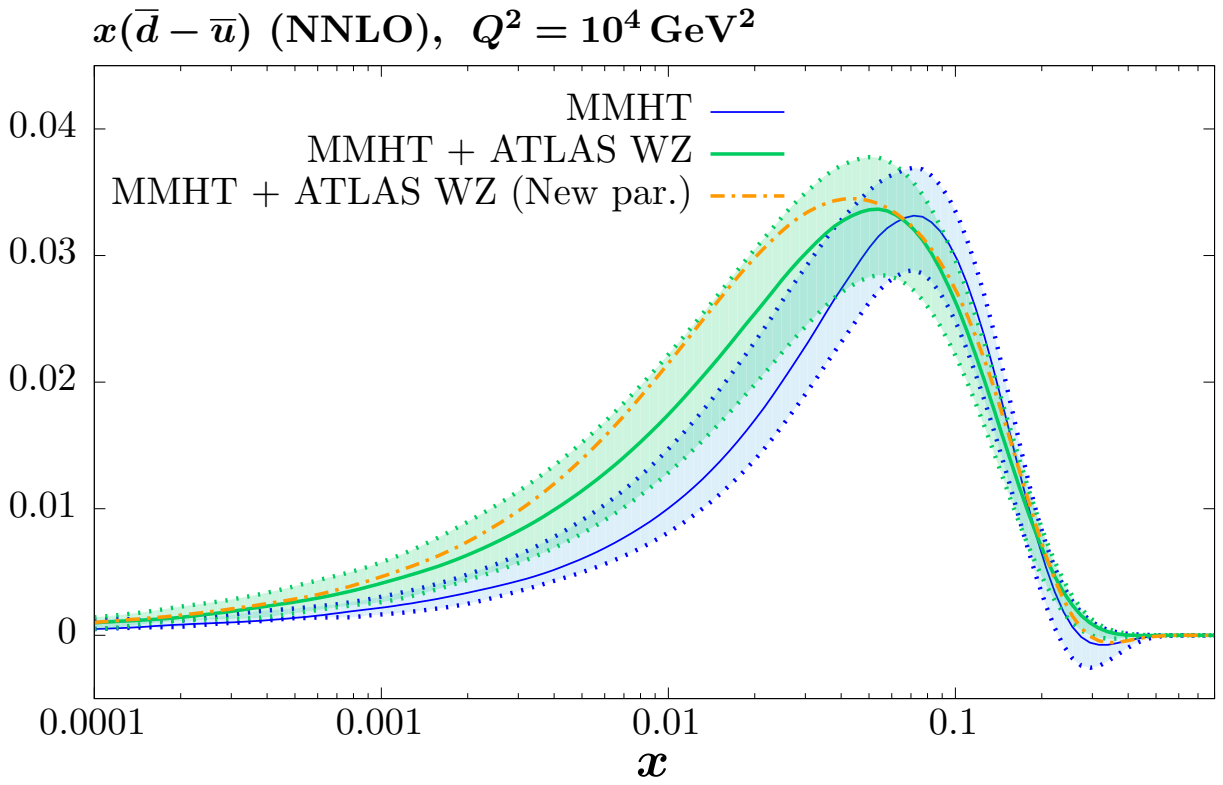

New $(\bar{d} - \bar{u})$ distribution similar at high x to previous one. (Dips to negative values at low-x allowed by, and seen using new parameterisation.)

Now a smaller decrease towards zero at low x beyond edge of previous uncertainty band.

Compared to Fitting Group Photons

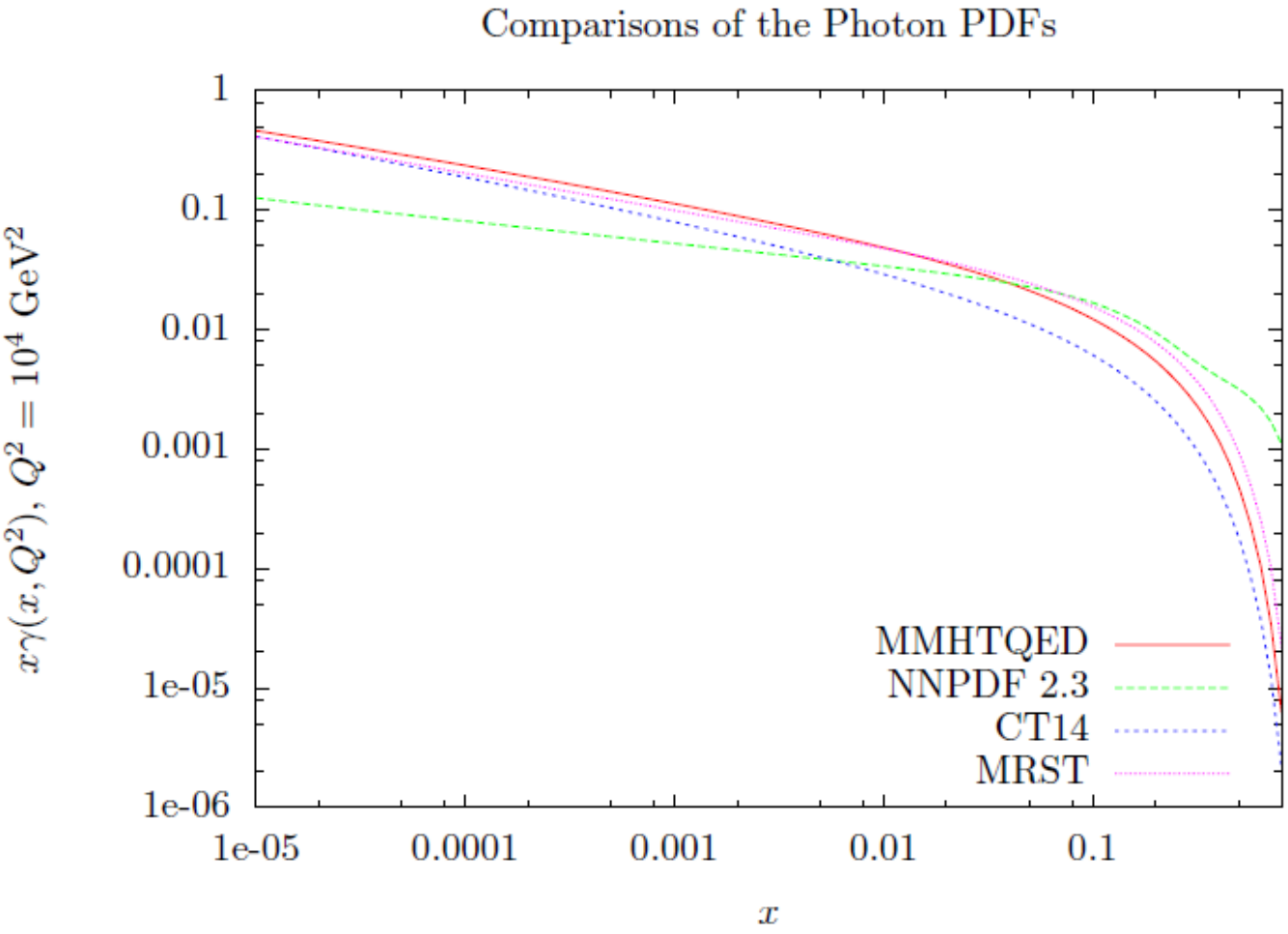

Smaller at high x than NNPDF and MRST.